

Supporting Information

Structure of the fungal hydroxylase, CYP505A30, and rational transfer of mutation data from CYP102A1 to alter regioselectivity

Jasmin C. Aschenbrenner,^{ab} Ana C. Ebrecht,^a Carmien Tolmie,^a Martha S. Smit,^{ab} and
Diederik J. Opperman^{*a}

Table of Contents

Section A. Material and Methods

1. Generation of CYP505A30 mutants.....	2
2. Data collection and structure determination.....	3

Section B. Supplementary Results

1. SDS-PAGE analysis of purified CYP505A30 HD.....	4
2. SDS-PAGE analysis of the expression levels of CYP505A30 and mutants.....	4
3. Average CYP450 content measured in whole cells, cell-free extract and in biotransformations.....	5
4. GC analysis of products from alkane biotransformations.....	6
4.1. Temperature programs for GC analysis of formed products.....	6
4.2. Standard curves.....	7
4.3. Chromatograms of biotransformations.....	8
4.4. Alcohol and diol production during hydroxylation of CYP505A30wt and mutants.....	15
5. Crystal structure of CYP505A30 HD.....	18

Section A. Material and Methods

1. Generation of CYP505A30 mutants

CYP505A30 mutants were generated using the Megaprimer method¹ with the primers stated in Table S1. The mutant CYP505A30_78-328_2 was generated from introducing the 78-328 mutations to CYP505A30_BM3wt. Megaprimer PCR reactions (50 μ L) consisted of 1X KOD Hot Start Polymerase buffer, 1.5 mM MgSO₄, 0.2 mM (each) deoxynucleoside triphosphates (dNTPs), 0.02 U·mL⁻¹ KOD Hot Start polymerase (Novagen), 0.4 ng·mL⁻¹ template DNA and 0.1 mM of both forward and reverse primers. PCR conditions consisted of an initial denaturation step (95 °C, 2 min), followed by 6 cycles of denaturation at 95 °C (20 s), annealing at 65 °C (10 s) and elongation at 70 °C (15 s) and 28 cycles of denaturation at 95 °C (20 s) and annealing and extension of the megaprimer at 70 °C (3:50 min) with a final extension of 12 min at 70 °C.

Table S1. Primers used for introducing mutations via the Megaprimer method.

Mutation	Construct Name	Forward Primer	Reverse Primer
F93V, I334F	87-328	CGATGGCCTCGTCACCGCTCG	GCTCGATTGATTATTGGGAACGTGGGACAGAGGC
V88A, I334A	BM3wt	CGAAACGGCGCCAACGATGGCC	GATTGATTATTGGGGCCGTGGGACAGAGGC
V84A, V88L, I334V	1-12G	CTCGCCGAGGCTCGAAACGGCCTGAACGATGGC	GCTCGATTGATTATTGGGACCGTGGGACAGAGGC

2. Data collection and structure determination

Table S2. X-ray data collection and refinement parameters.

Data collection	
Beamline	i04
Wavelength (Å)	0.9795
Space group	P4 ₂ 2 ₁ 2
Cell dimensions a/b/c (Å)	171.49/171.49/175.65
$\alpha/\beta/\gamma$ (°)	90/90/90
Resolution (Å)	61.35 - 2.33 (2.37 - 2.33)
Unique reflections	111842 (5522)
Completeness (%)	100.0 (95.9)
Mn(I)/sd(I)	16.2 (0.2)
Multiplicity	13.3 (13.1)
R _{merge}	0.085 (4.010)
R _{pim}	0.024 (1.154)
CC _{1/2}	1.000 (0.296)
Molecules in ASU	4
Refinement	
R _{work} /R _{free}	0.2033/0.2339
Number of residues modelled	1832
B-factors	
Amino acids	89.11
Ligands	78.51
Waters	71.64
Rmsd Bond lengths (Å)	0.0099
Rmsd Bond angles (°)	1.6466
Ramachandran distribution (%) (favoured/allowed/outliers)	96.1/3.1/0.8
MolProbity score	1.86
Poor rotamers (%)	4.45
Clash score, all atoms	3.03
PDB ID	7P6L

Values in parantheses describe the outer shell.

Section B. Supplementary Results

1. SDS-PAGE analysis of purified CYP505A30 HD

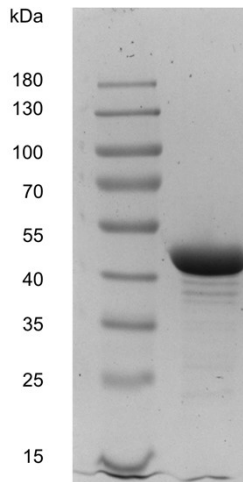


Figure S1. SDS-PAGE of CYP505A30 HD (54.7 kDa) after purification with immobilized metal affinity chromatography and size exclusion chromatography.

2. SDS-PAGE analysis of the expression levels of CYP505A30 and mutants

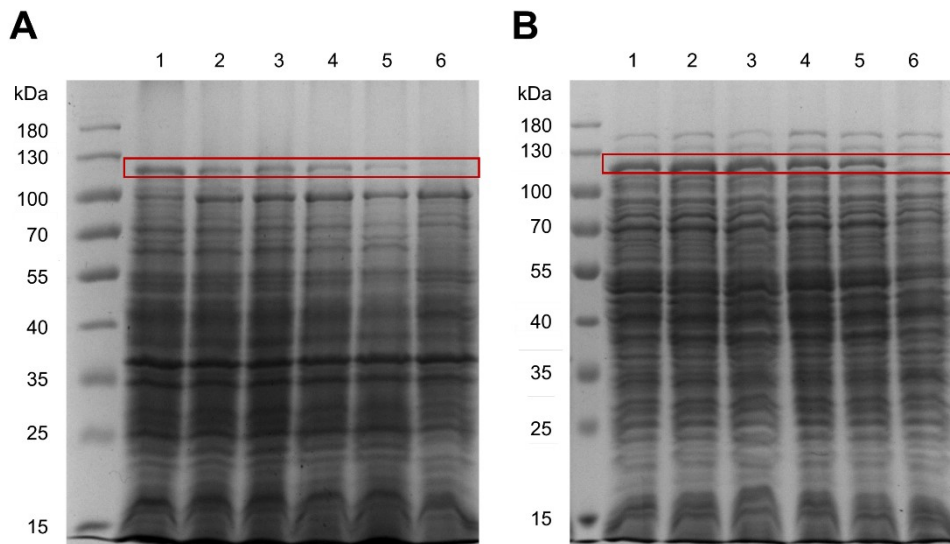


Figure S2. SDS-PAGE analysis of the crude (A) and cell-free extract (B) prepared from *E. coli* BL21-DE3 (Gold) cells transformed with pET22b(+)-plasmids expressing the (1) CYP505A30wt, (2) CYP505A30_BM3wt, (3) CYP505A30_1-12G, (4) CYP505A30_87-328 (5) CYP505A30_87-328_2 or transformed with (6) an empty pET22b(+)-plasmid. The predicted molecular weight of the expressed proteins is approximately 120 kDa.

3. Average CYP450 content measured in whole cells, cell-free extract and in biotransformations

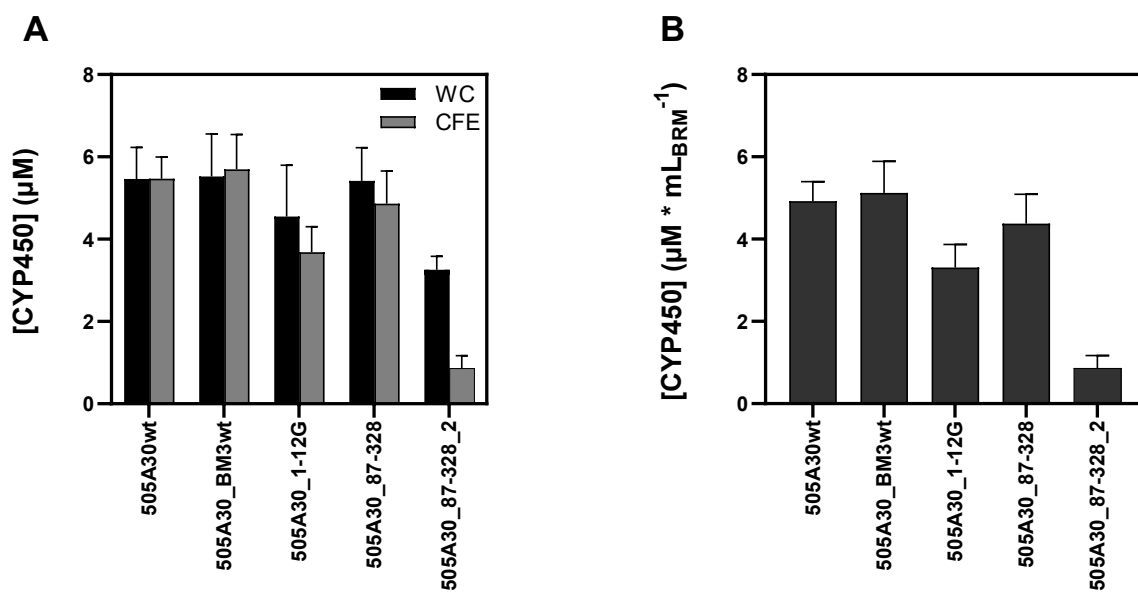


Figure S3. (A) Comparison of CYP450 content in whole cell (WC) and CFE with a constant wet cell biomass of 1 g in 5 ml buffer measured in duplicates from 5 different experiments. (B) Average CYP450 content in CFE BRM.

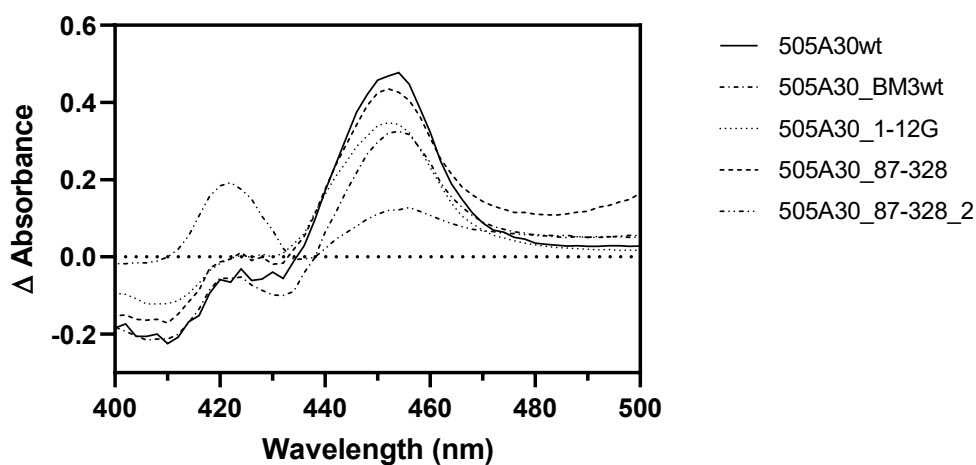


Figure S4. Representative examples of CO-difference spectra obtained by CYP505A30wt and mutants in CFE with a constant wet cell biomass of 1 g in 5 ml buffer.

4. GC analysis of products from alkane biotransformations

4.1. Temperature programs for GC analysis of formed products

Table S3. GC programs for the analysis of products formed during biotransformations. The products were analysed on a Finnigan TRACE GC Ultra (Thermo Fisher Scientific). Samples were silylated for analysis and quantification of diols.

Analysis	Derivatization	Column	Program	Compound	Retention time [min]
GC	none	FactorFour VF-5ms column (60 m x 0.32 mm x 0.25 µm, Varian)	50/2/3/75/0/15/190/0/[^a]	4-Octanol	8.98
				3-Octanol	9.22
				2-Octanol	9.41
				2,5-Octanediol	13.97
				3,6-Octanediol	14.07
				2,6-Octanediol	14.26
				2,7-Octanediol	14.33
				1-Undecanol[^c]	16.29
GC	BSTFA	FactorFour VF-5ms column (60 m x 0.32 mm x 0.25 µm, Varian)	100/1/10/300/5/[^b]	2,5-Octanediol	6.14
				3,6-Octanediol	6.24
				2,6-Octanediol	6.50
				2,7-Octanediol	6.72
				1,8-Octanediol	8.51
				1-Undecanol[^c]	7.76
GC	none	BPX90 (30 m x 0.25 mm x 0.25 µm)	80/2/15/280/4.66/[^b]	4-Decanol	3.71
				3-Decanol	3.80
				2-Decanol	3.99
				1-Dodecanol[^c]	6.17
				2,7-Decanediol	8.62
				2,8-Decanediol	8.92
				2,9-Decanediol	9.06
				3,8-Decanediol	8.73
GC	BSTFA	FactorFour VF-5ms column (60 m x 0.32 mm x 0.25 µm, Varian)	100/1/10/300/5/[^b]	2,7-Decanediol	8.62
				3,8-Decanediol	8.73
				2,8-Decanediol	8.92
				2,9-Decanediol	9.13
				1,10-Decanediol	10.91
				1-Dodecanol[^c]	9.00
GC	none	Astec CHIRALDEX™ G-TA column (30 m x 0.25 mm x 0.12 µm)	40/20/0.75/70/0/[^b]	(S)-2-Octanol	45.4
				(R)-2-Octanol	45.7

[^a] Initial temp (°C)/ time (min)/ slope (°C/min)/ temperature (°C)/ hold time (min)/ slope (°C/min)/ temperature (°C)/ hold time (min), [^b] Initial temp (°C)/ time (min)/ slope (°C/min)/ temperature (°C)/ hold time (min), [^c] Internal standard

4.2. Standard curves

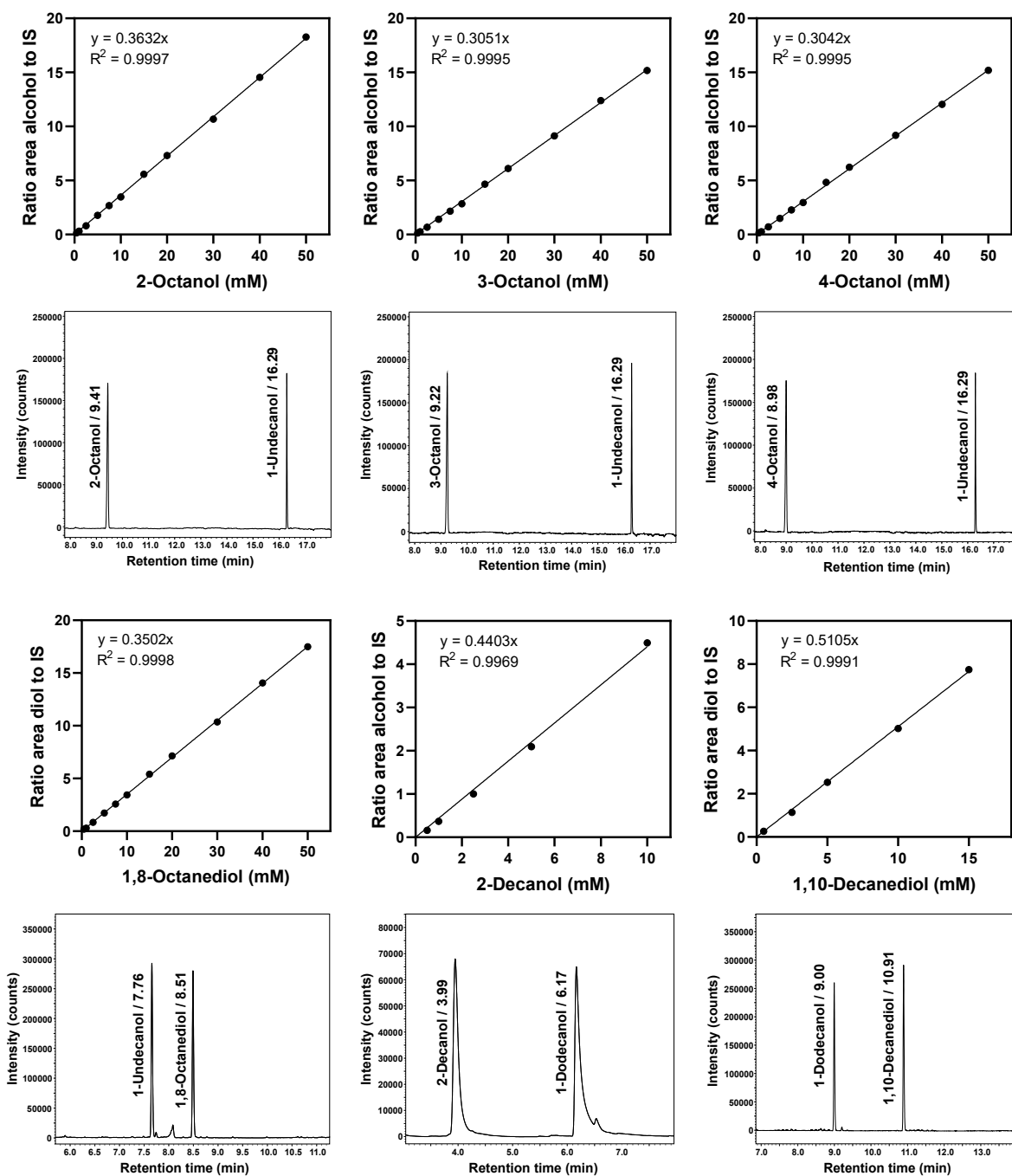


Figure S5. Calibration curves and GC chromatograms for the standards. Concentrations of produced alcohols (*n*-octanol and *n*-decanol) were determined from standard curves of 2-, 3- and 4-octanol as well as 2-decanol. Diol concentrations were calculated from 1,8-octanediol and 1,10-decanediol standard curves.

4.3. Chromatograms of biotransformations

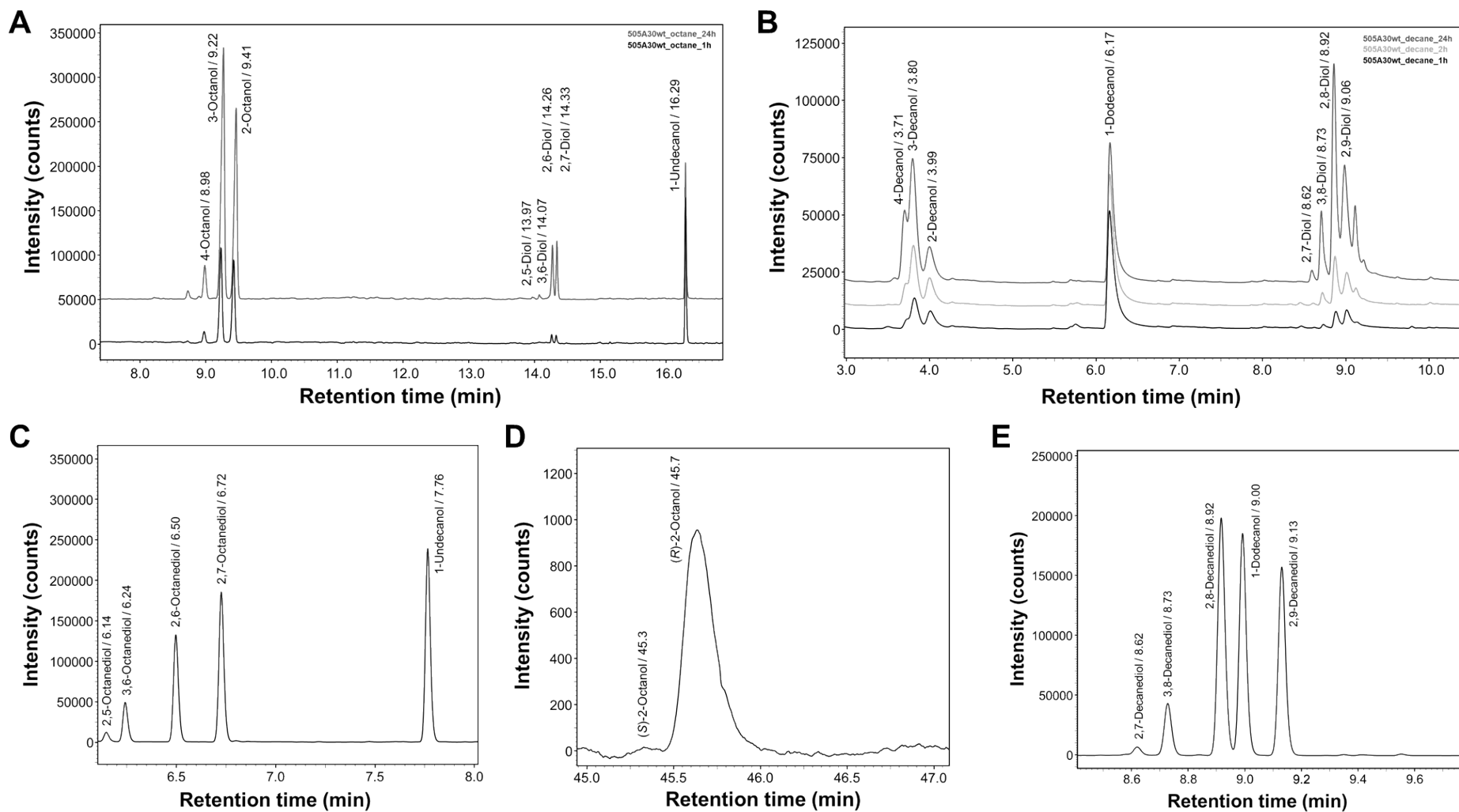


Figure S6. Representative examples of GC chromatograms of biotransformations with CYP505A30wt. GC chromatograms of (A) octane biotransformations at 1 h and 24 h and (B) decane biotransformations at 1 h, 2 h and 24 h. GC chromatograms of silylated samples for diol analysis from octane (C) and decane (E) after 24 h. (D) GC chromatogram of chiral analysis of 1 h sample of octane biotransformations.

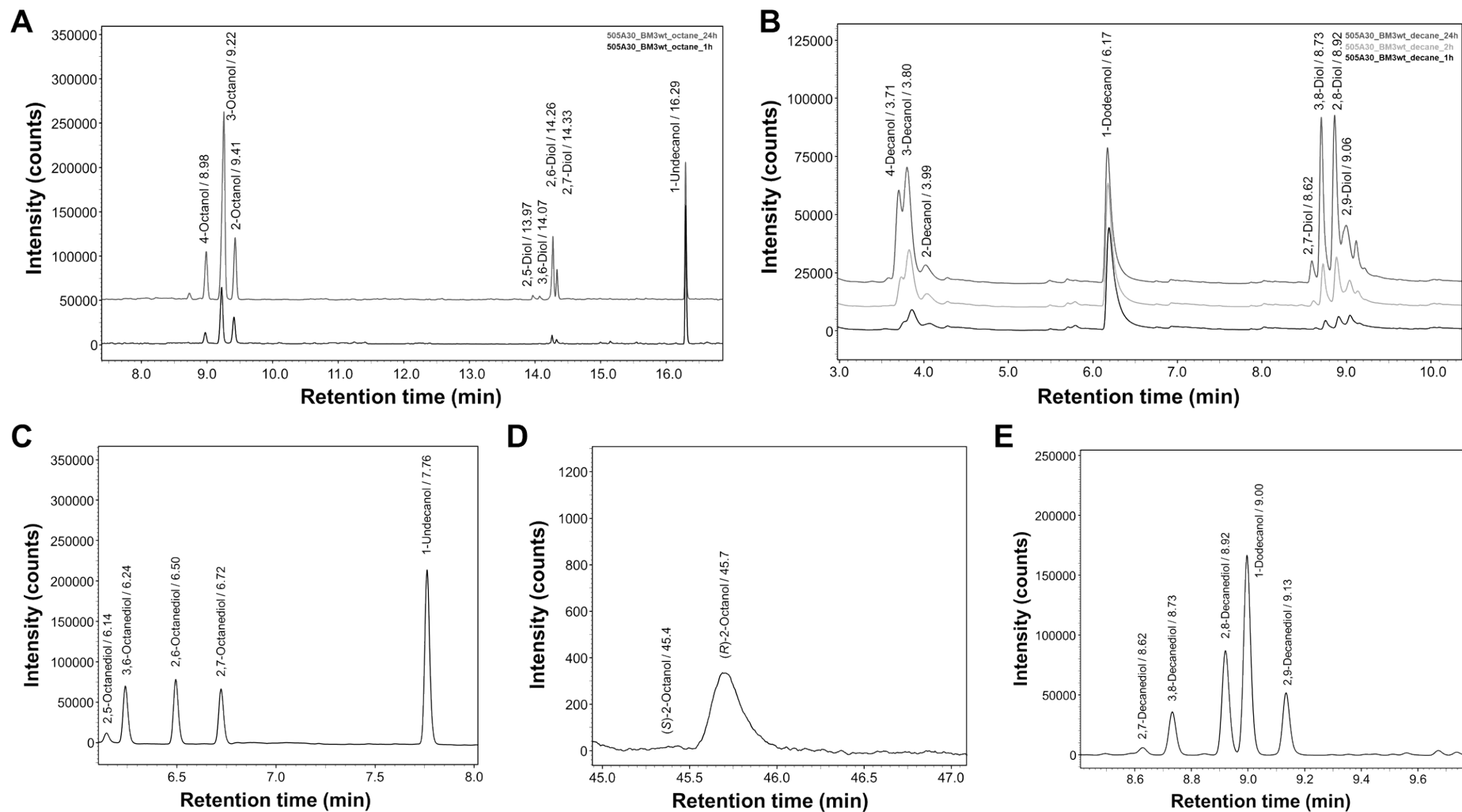


Figure S7. Representative examples of GC chromatograms of biotransformations with CYP505A30_BM3wt. GC chromatograms of (A) octane biotransformations at 1 h and 24 h and (B) decane biotransformations at 1 h, 2 h and 24 h. GC chromatograms of silylated sample for diol analysis from octane (C) and decane (E) after 24 h. (D) GC chromatogram of chiral analysis of 1 h sample of octane biotransformations.

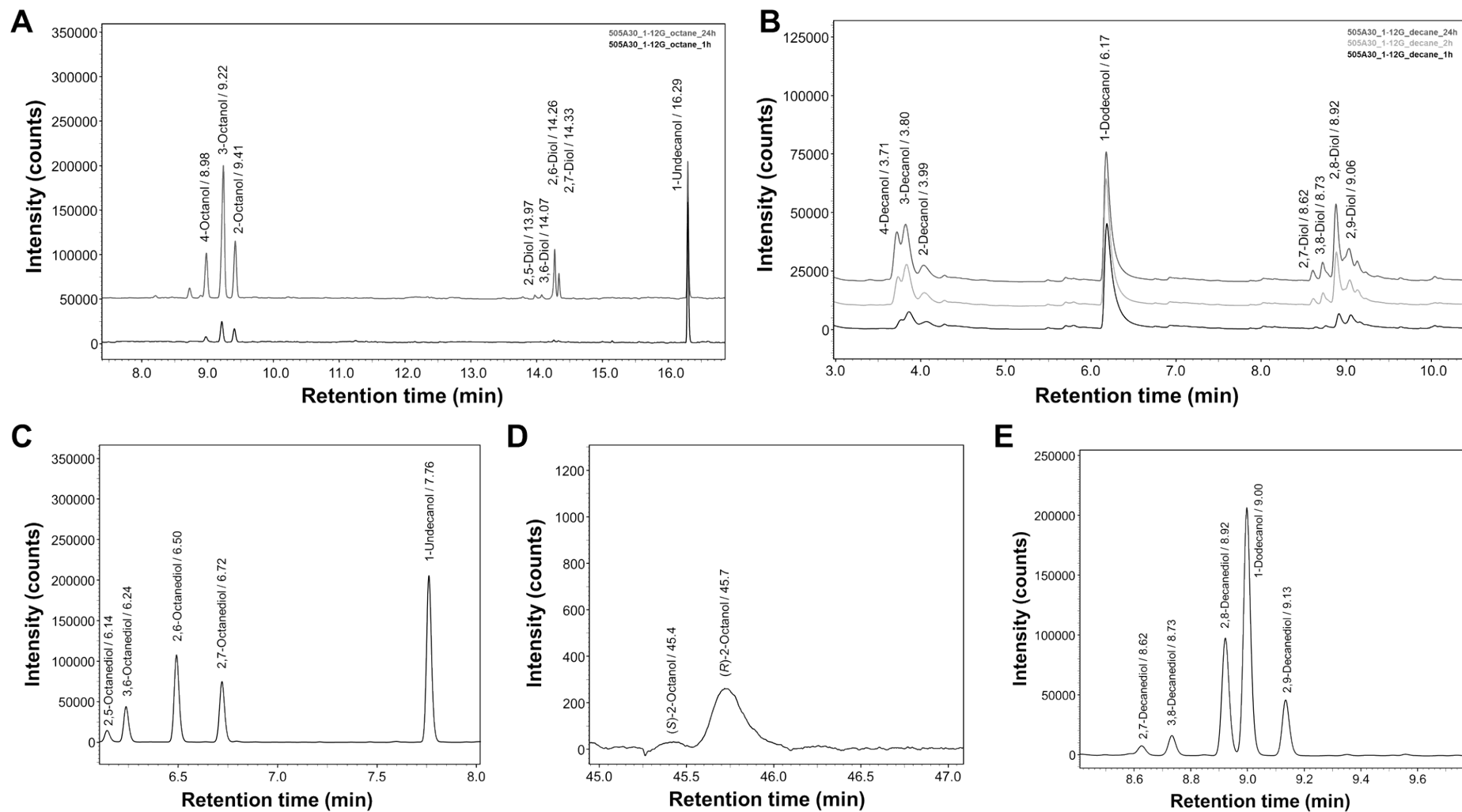


Figure S8. Representative examples of GC chromatograms of biotransformations with CYP505A30_1-12G. GC chromatograms of (A) octane biotransformations at 1 h and 24 h and (B) decane biotransformations at 1 h, 2 h and 24 h. GC chromatograms of silylated sample for diol analysis from octane (C) and decane (E) after 24 h. (D) GC chromatogram of chiral analysis of 1 h sample of octane biotransformations.

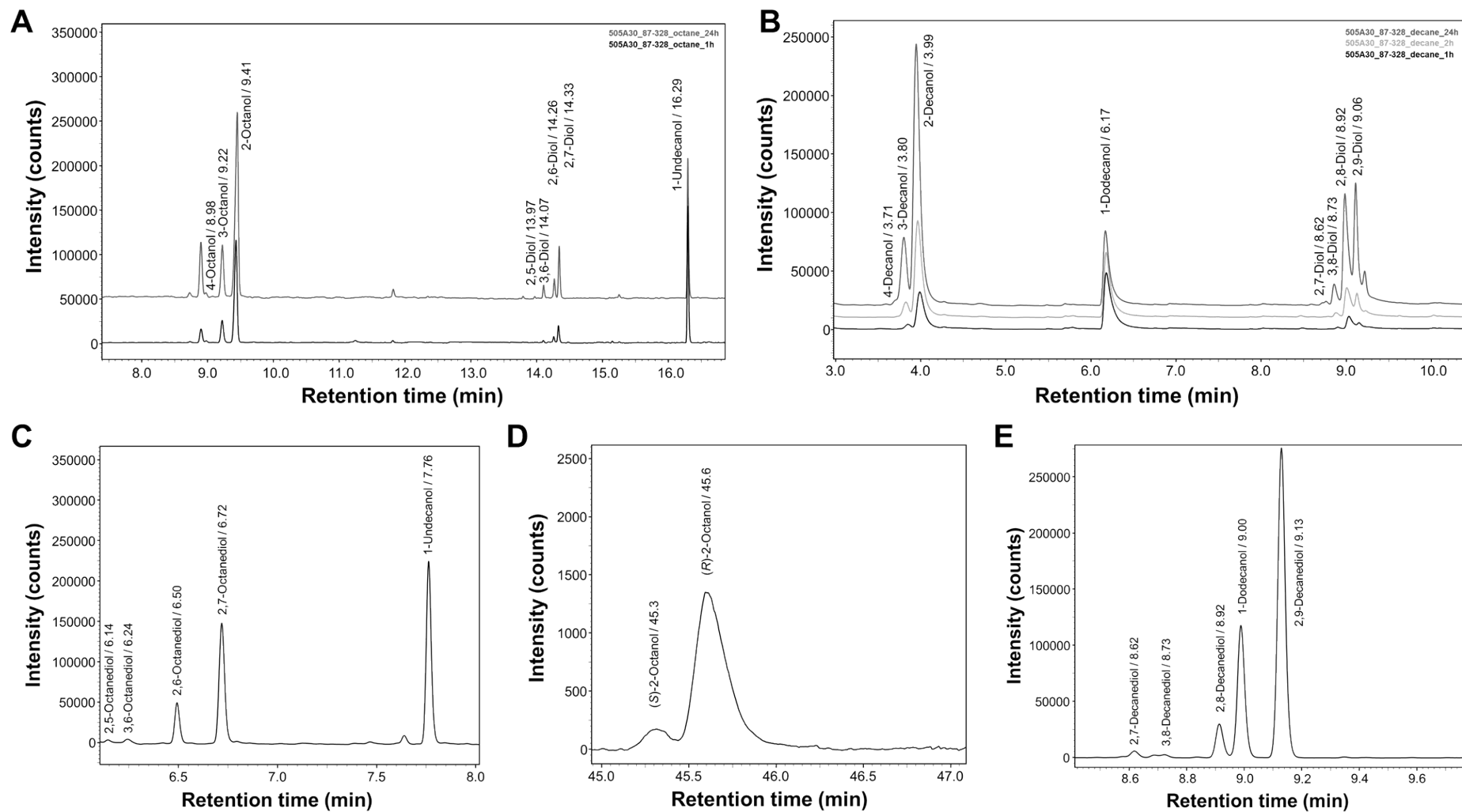


Figure S9. Representative examples of GC chromatograms of biotransformations with CYP505A30_87-328. GC chromatograms of (A) octane biotransformations at 1 h and 24 h and (B) decane biotransformations at 1 h, 2 h and 24 h. GC chromatograms of silylated sample for diol analysis from octane (C) and decane (E) after 24 h. (D) GC chromatogram of chiral analysis of 1 h sample of octane biotransformations.

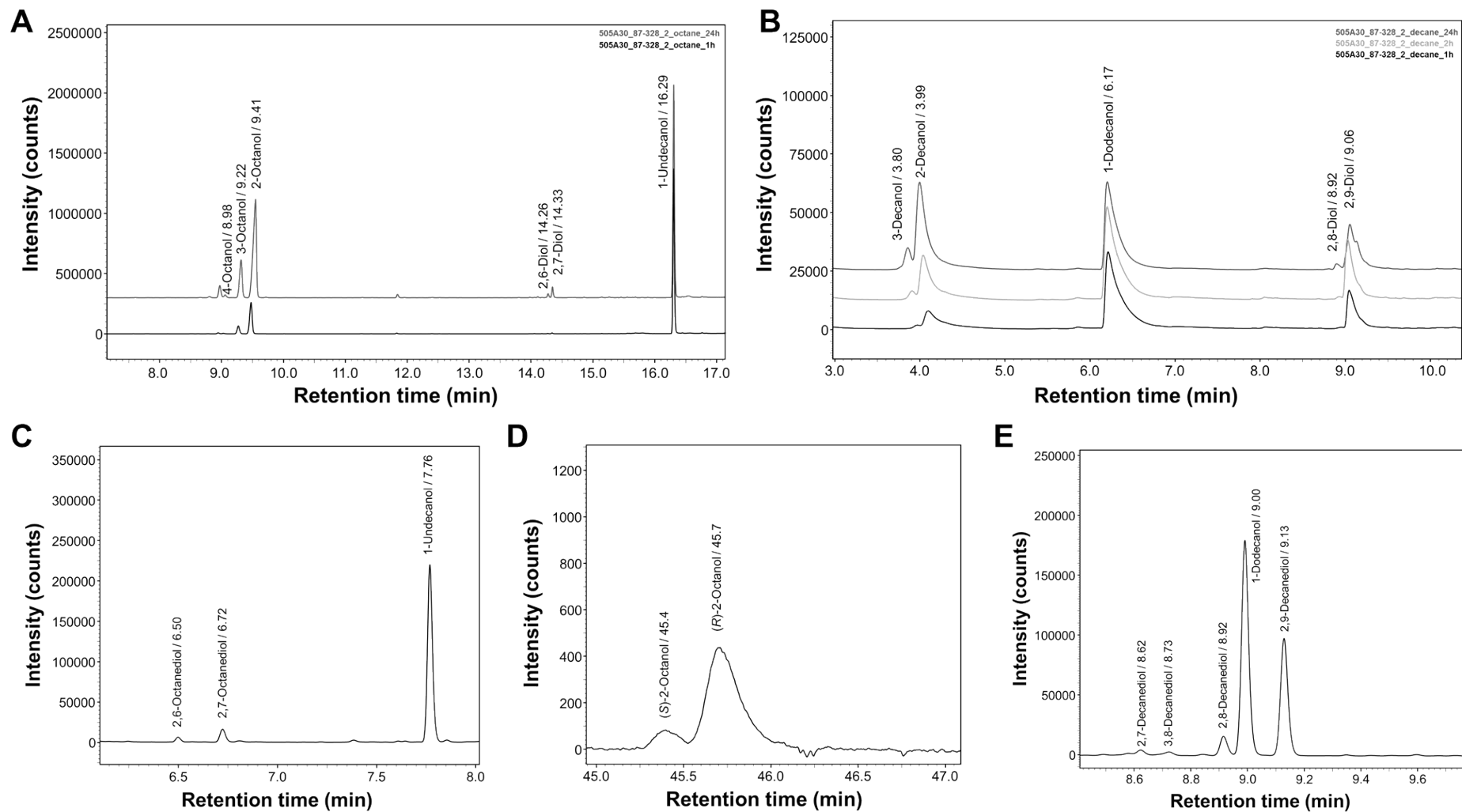


Figure S10. Representative examples of GC chromatograms of biotransformations with CYP505A30_87-328_2. GC chromatograms of (A) octane biotransformations at 1 h and 24 h and (B) decane biotransformations at 1 h, 2 h and 24 h. GC chromatograms of silylated sample for diol analysis from octane (C) and decane (E) after 24 h. (D) GC chromatogram of chiral analysis of 1 h sample of octane biotransformations.

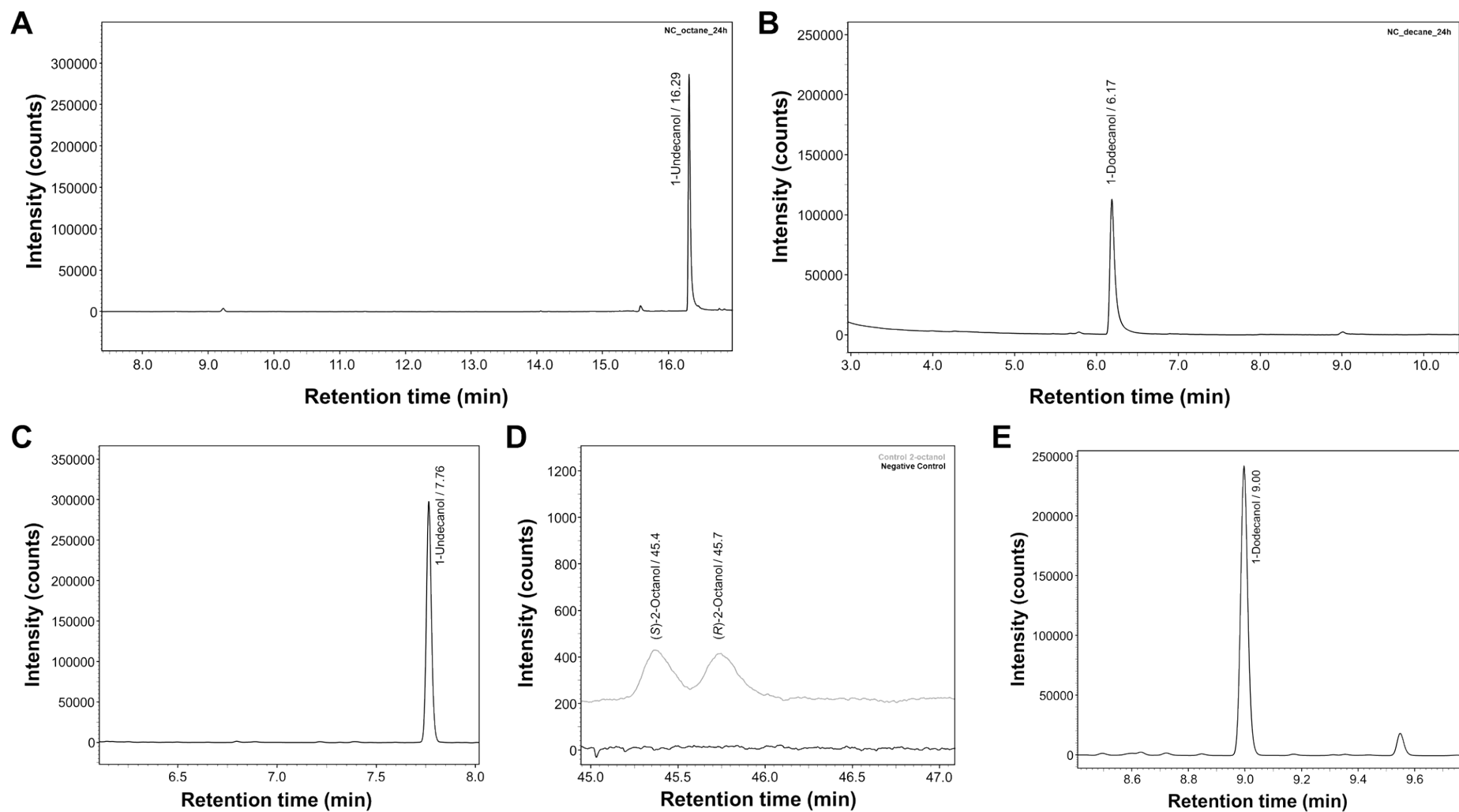


Figure S11. Representative examples of GC chromatograms of biotransformations of the negative control. GC chromatograms of (A) octane biotransformations at 1 h and 24 h and (B) decane biotransformations at 1 h, 2 h and 24 h. GC chromatograms of silylated sample for diol analysis from octane (C) and decane (E) after 24 h. (D) GC chromatogram of chiral analysis of a racemic 2-octanol sample.

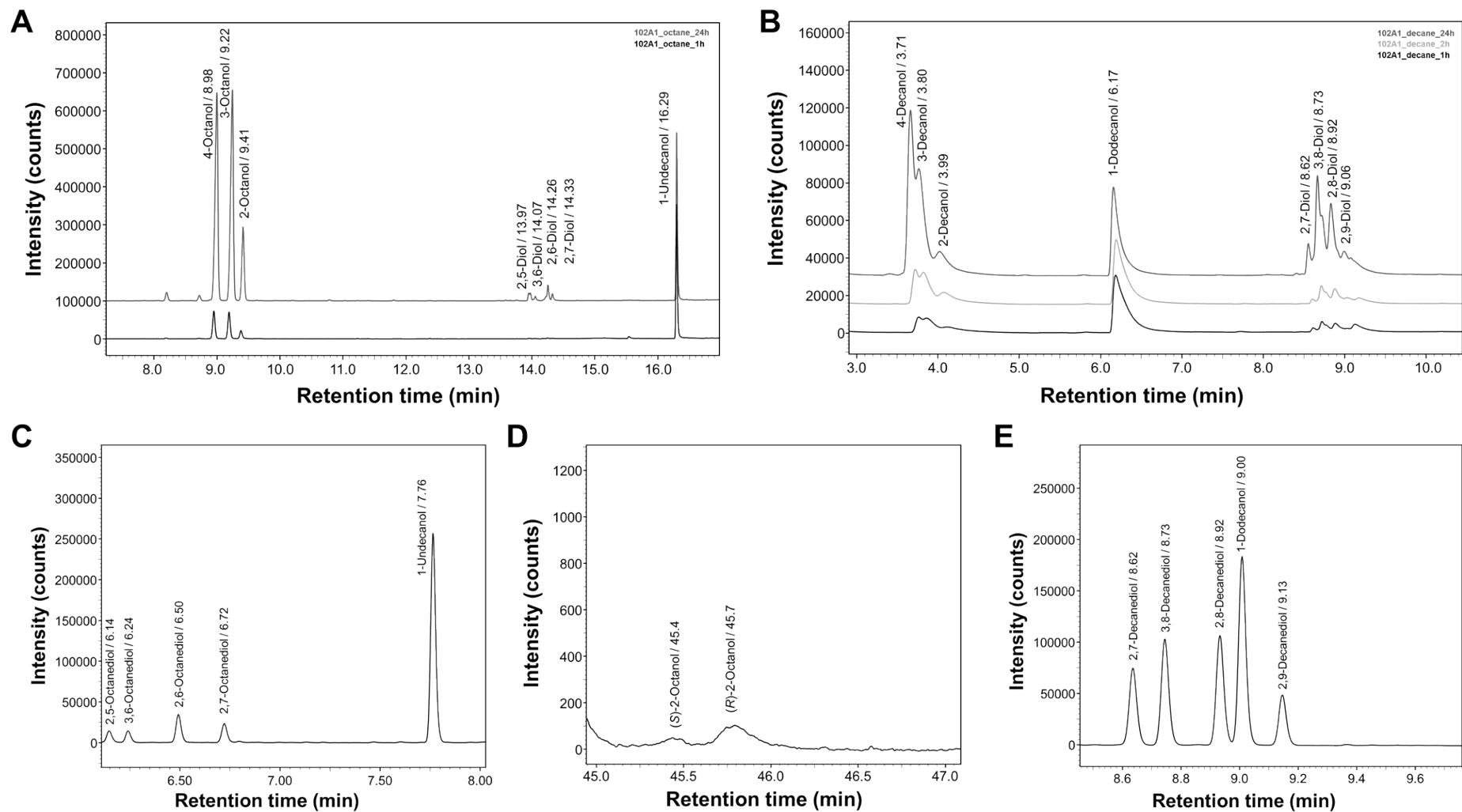


Figure S12. Representative examples of GC chromatograms of biotransformations with CYP102A1. GC chromatograms of (A) octane biotransformations at 1 h and 24 h and (B) decane biotransformations at 1 h, 2 h and 24 h. GC chromatograms of silylated sample for diol analysis from octane (C) and decane (E) after 24 h. (D) GC chromatogram of chiral analysis of 1 h sample of octane biotransformations.

4.4. Alcohol and diol production during hydroxylation of CYP505A30 and mutants

Table S4. Total turnover numbers (TTN) for CYP505A30 (Wt) and mutants in comparison to TTN determined by Pennec *et al.*² on CYP102A1 and its variants. Diol formation was not considered in CYP102A1 data².

Mutation	Octane		Decane	
	our work	respective 102A1 variants	our work	respective 102A1 variants
505A30wt	7860 ± 1580		2730 ± 480	
505A30_BM3wt	4390 ± 1060	2090	2300 ± 230	1490
505A30_1-12G	4720 ± 1520	2630	1500 ± 310	540
505A30_87-328	3670 ± 910	370	3160 ± 960	150
505A30_87-328_2	4660 ± 960	370	4120 ± 350	150

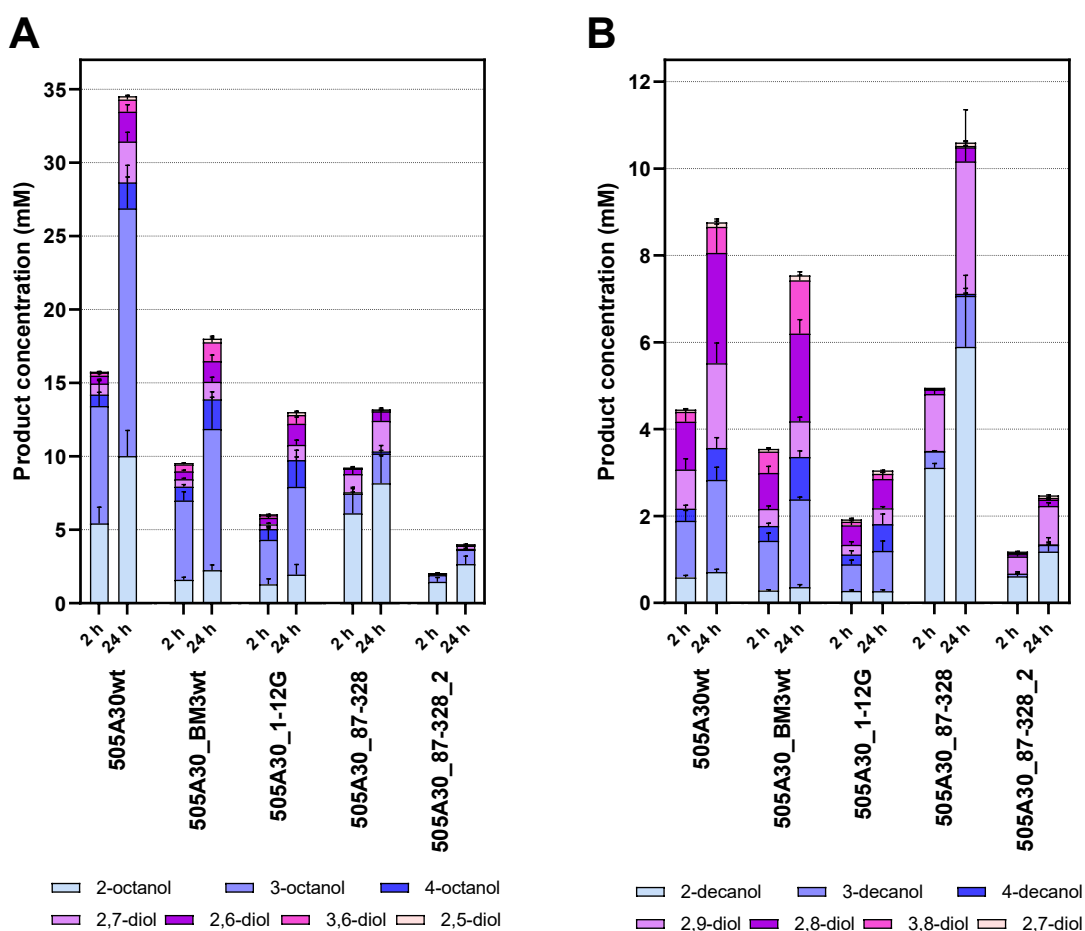


Figure S13. Product formation of CYP505A30wt and mutants at 2 h and 24 h of biotransformations of octane (A) and decane (B) based on the average CYP concentration achieved in the BRM.

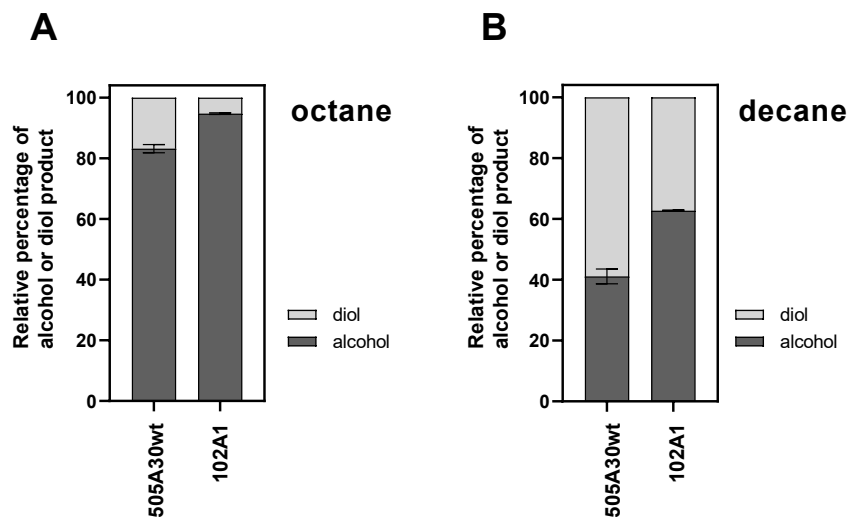


Figure S14. Relative percentage of alcohol and diol product formation of CYP505A30wt and CYP102A1 at 24 h of biotransformations of octane (A) and decane (B) with substrate added in excess. [CYP505A30] = 5 μ M, [CYP102A1] = 13 μ M.

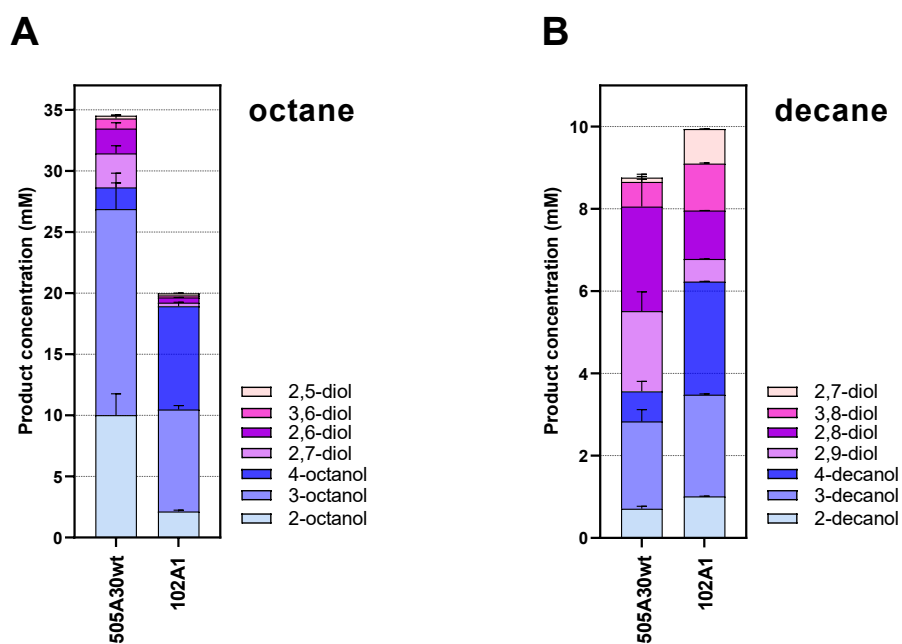


Figure S15. Product formation of CYP505A30wt and CYP102A1 at 24 h of biotransformations of octane (A) and decane (B) with substrate added in excess. [CYP505A30] = 5 μ M, [CYP102A1] = 13 μ M.

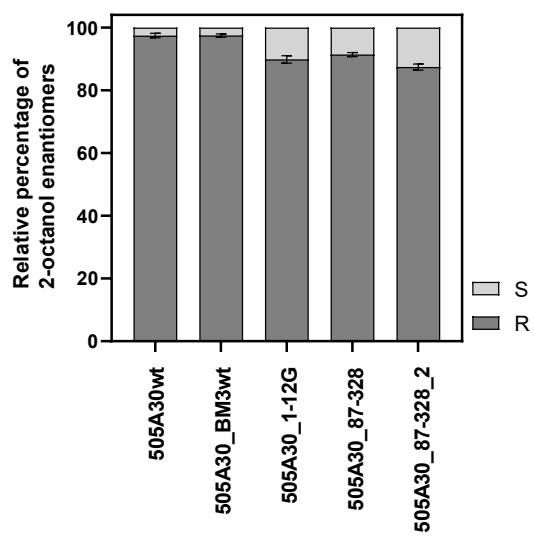


Figure S16. Chiral analysis of 2-octanol enantiomers formed by CYP505A30wt and mutants. 1 h data points were analysed and plotted.

5. Crystal structure of CYP505A30 HD

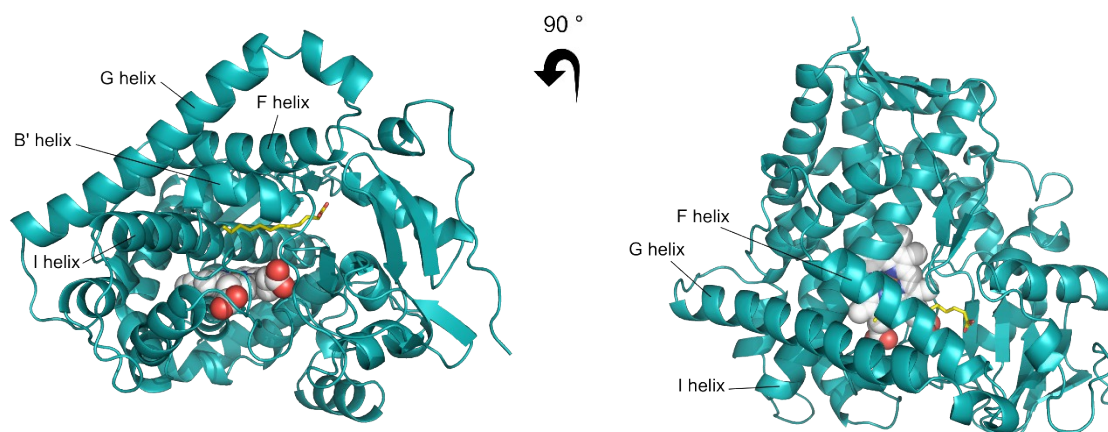


Figure S17. Crystal structure of CYP505A30 HD reveals the typical closed fold of CYP450s crystallised with substrate. The haem, shown as spheres, is bound to a conserved cysteine, and the substrate dodecanoic acid is highlighted in yellow.

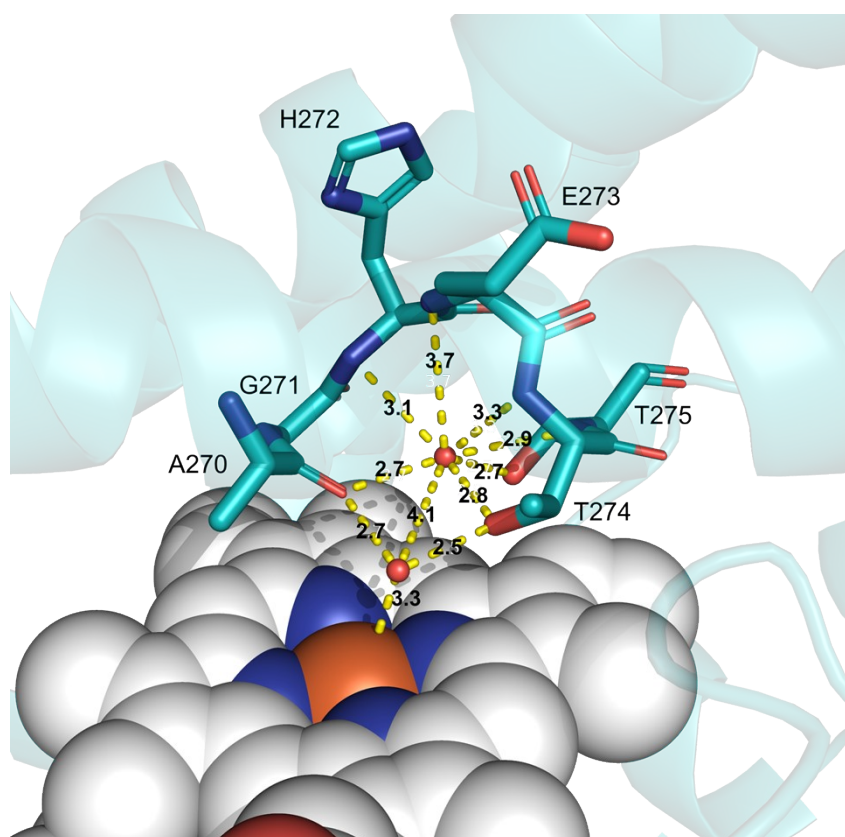


Figure S18. I-helix of CYP505A30 HD showing the catalytically important acid-alcohol pair (E273 and T274) and the coordinated water molecules including the hydrogen bonding network.

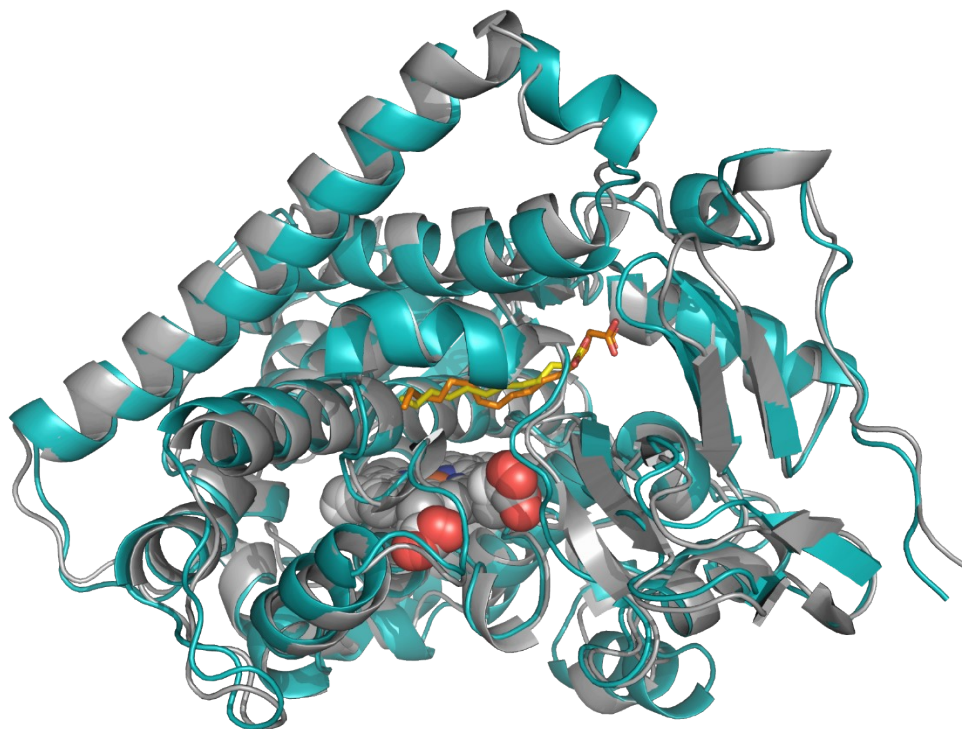


Figure S19. Overlay of the crystal structures of CYP505A30 HD (cyan) with dodecanoic acid (yellow) and CYP102A1 (PDB 1fag, grey) with palmitoleic acid (orange) shows a high similarity of the overall structure.

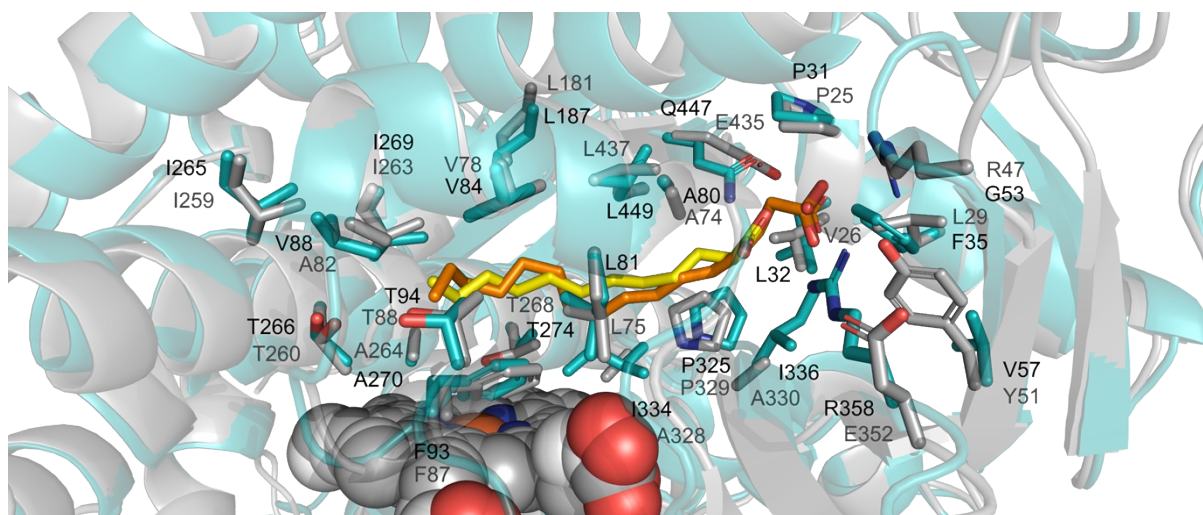


Figure S20. Overlay of the active site of CYP505A30 HD (green) with dodecanoic acid (yellow) with the active site of CYP102A1 (PDB 1fag, grey) with palmitoleic acid (orange). 7 residues are located within 4 Å of the substrate in CYP505A30, including F35, F93, I269, I334, I336, R358, L449.

References

- 1 J. Sanchis, L. Fernández, J. D. Carballeira, J. Drone, Y. Gumulya, H. Höbenreich, D. Kahakeaw, S. Kille, R. Lohmer, J. J. P. Peyralans, J. Podtetenieff, S. Prasad, P. Soni, A. Taglieber, S. Wu, F. E. Zilly and M. T. Reetz, *Appl. Microbiol. Biotechnol.*, 2008, **81**, 387–397.
- 2 A. Pennec, C. L. Jacobs, D. J. Opperman and M. S. Smit, *Adv. Synth. Catal.*, 2015, **357**, 118–130.